



Evaluation of UV Photolysis of Formaldehyde in a Continuous Flow Reactor with Different Diffusive Glass Plates

Avaliação da fotólise UV de formaldeído em reator de fluxo contínuo com diferentes placas vítreas difusoras

- **Data de entrada:**
09/04/2024
- **Data de aprovação:**
18/02/2026

Thiago Marendra Rosa de Lima¹ | Nikolai Otto² | Alvaro Luiz Mathias^{1*}

DOI: <https://doi.org/10.36659/dae.2026.128>

Lima TMR  <https://orcid.org/0009-0006-6793-3552>
Otto N  <https://orcid.org/0000-0001-8828-3022>

Mathias AL  <https://orcid.org/0000-0003-2536-4516>

Abstract

This study evaluated the degradation of formaldehyde in aqueous solution by ultraviolet (UV) and homogeneous photolysis with hydrogen peroxide (UV/H₂O₂) in a plug flow reactor and validated an analytical method based on the chromotropic acid reaction for process monitoring. The method showed high sensitivity and linearity of 0.10–4.00 mg·L⁻¹ (R² = 0.9973), with a 0.126 mg·L⁻¹ detection limit and a 0.382 mg·L⁻¹ quantification limit. The characteristic purple color remained intense and stable under concentrated H₂SO₄ (98%). The method showed high precision (CV = 1.58%; ΔAbs% < 5.00%), confirming its suitability for controlled kinetic and photolytic assays. However, due to multiple interferents, the technique is only applicable to formaldehyde solutions under chemically controlled conditions using high-purity reagents, and it is not recommended for real effluents. Photolysis efficiency was strongly influenced by pH and diffuser material. At neutral pH, UV photolysis achieved up to 12.72% removal (Bosil plate) and UV/H₂O₂, up to 7.27%. Under acidic conditions (≈2.3), chemical oxidation with H₂O₂ reached 14.45% and UV/H₂O₂ achieved 24.19% (BosilF60) removal, indicating a synergistic effect. Borosilicate plates (Bosil and BosilF60) outperformed soda-lime glass ones, highlighting the importance of optimizing the solid-radiation optical interface. The results show the technical feasibility of combining robust analytical methods with continuous photochemical processes for formaldehyde removal.

Keywords: Formaldehyde. Chromotropic acid. UV photolysis. Chemical oxidation. Plug flow reactor (PFR). Wastewater treatment.

Resumo

Este estudo avaliou a degradação de formaldeído em solução aquosa por fotólise UV (UV) e fotólise homogênea assistida por peróxido de hidrogênio (UV/H₂O₂) em reator de escoamento pistão (PFR), bem como validou o método analítico baseado na reação cromotrópica para monitoramento do processo. O método apresentou alta sensibilidade e linearidade entre 0,10 e 4,00 mg·L⁻¹ (R² = 0,9973), limite de detecção de 0,126 mg·L⁻¹ e quantificação de 0,382 mg·L⁻¹. A coloração púrpura característica foi intensa e estável com H₂SO₄ concentrado (98%). A precisão foi elevada (CV = 1,58%; ΔAbs% < 5,00%), confirmando a adequação do método para ensaios cinéticos e fotolíticos controlados. No entanto, devido a múltiplos interferentes, a técnica é aplicável apenas a soluções de formaldeído em meio quimicamente controlado com reagentes de alta pureza, não sendo indicada

¹ Federal University of Paraná – Curitiba – Paraná – Brazil.

² University of Stuttgart – Stuttgart – Germany

* **Correspondent author:** mathias@ufpr.br

para efluentes reais. A eficiência da fotólise dependeu fortemente do pH e do material difusor. Em pH neutro, a fotólise UV removeu até 12,72% (placa Bosil), e UV/H₂O₂ até 7,27%. Em pH ácido (≈2,3), a oxidação química com H₂O₂ atingiu 14,45%, e UV/H₂O₂ chegou a 24,19% (BosilF60), evidenciando efeito sinérgico. Placas de borossilicato (Bosil e BosilF60) superaram as de soda-cal, destacando a importância da otimização óptica da interface sólido–radiação. Os resultados demonstram a viabilidade técnica do uso conjunto de métodos analíticos robustos e processos fotoquímicos contínuos para remoção de formaldeído.

Palavras-chave: Ácido cromotrópico. Fotólise UV. Oxidação química. Reator de fluxo pistão (PFR). Tratamento de efluente.

1 INTRODUCTION

Formaldehyde (HCHO), a low-molecular-weight carbonyl compound (30.03 g·mol⁻¹), widely occurs in the environment due to its formation via natural processes and various human activities (Johari *et al.*, 2018). It is used in the manufacture of construction materials and personal care products (Bessaire *et al.*, 2018; Ghani *et al.*, 2018; Johari *et al.*, 2018) and as a food preservative in fish, seafood, oils, and fats (Nurlely *et al.*, 2021). Its high solubility in water (≈400 g·L⁻¹ at 20 °C), ethanol, and chloroform and its miscibility with acetone, benzene, and diethyl ether (Kaden *et al.*, 2010) facilitate its dispersion and increase potential environmental and health risks. These risks underscore the need to understand its properties, toxicity, and control strategies (Delikhoon *et al.*, 2018; Reingruber; Pontel, 2018; Yu *et al.*, 2019).

In aquatic environments, formaldehyde may occur from trace levels to gram-per-liter concentrations, being toxic to aquatic organisms above 5 mg·L⁻¹ (Gonzalez-Gil; Kleerebezem; Lettinga, 2002). It has also been detected in drinking water, such as in Tanzania (2.46–19.25 µg·L⁻¹; Lugwisha; Mahugija; Mwankuna, 2016) and in ozonated distribution systems (up to 30 µg·L⁻¹; World Health Organization – WHO, 2005). Several treatment technologies have been investigated, including aerobic and anaerobic biological processes, chemical oxidation with O₃ or H₂O₂, and wet catalytic oxidation (Vakylabad, 2021). Among advanced oxidation processes, CSTR, PBR, and

plug-flow reactors (PFR) are widely employed. PFRs are particularly suitable for homogeneous photolysis due to their steady-state operation and high conversion efficiency.

This study evaluated photolysis in a PFR using five diffuser plates—three borosilicate and two soda-lime glass ones—serving as UV-transmitting and diffusing surfaces for LED irradiation, thus enabling the comparison of the optical properties of the glass materials regarding formaldehyde degradation. The hydroxyl radical generated by high-intensity UV photolysis or by homogeneous photolysis assisted by H₂O₂ is the main oxidizing agent given its high reactivity and redox potential (+2.8 V), which exceeds that of ozone, hydrogen peroxide, chlorine dioxide, and chlorine (Dalponte *et al.*, 2016). H₂O₂ can also directly oxidize formaldehyde, forming formic acid under acidic conditions or formate under alkaline conditions (Mattos *et al.*, 2003) and acting as a precursor of hydroxyl radicals. This study also explored several oxidative routes: UV photolysis at neutral pH (UV pH=7.0), UV photolysis assisted by H₂O₂ at neutral pH (UV pH=7.0 H₂O₂), and UV photolysis assisted by H₂O₂ under acidic conditions (UV pH=2.3 H₂O₂).

Formaldehyde determination in water requires a chromophoric reagent due to the overlap between its absorption bands (100–270 nm and < 185 nm) and the strong absorption of water in the deep UV region (Larsen, 2024). Techniques such as HPLC, GC–MS, and UV–Vis spectrophotometry can be applied (Nurlely *et al.*, 2021), with HPLC and

UV-Vis being the most widely used (Hladová *et al.*, 2019). UV-Vis spectrophotometry is simple and sensitive (Gasparini *et al.*, 2008), and its response can be tuned by adjusting the optical path length (Sawicki; Hauser; McPherson, 1962). Among the available chromogenic reagents, chromotropic acid stands out for its sensitivity, selectivity, and stability, reacting with formaldehyde under strongly acidic conditions (Shariati-Rad; Irandoust; Mozaffarinia, 2016).

This study evaluated the suitability of this method to monitor formaldehyde degradation under the conditions of a PFR system, including variations in pH, diffuser-plate optical properties, and the presence of H₂O₂. The used concentration (20 mg·L⁻¹) closely resembles that reported in a catalytic ozonolysis study using TiO₂ (5 mg·L⁻¹; Cui *et al.*, 2011), thereby enabling a comparison with the AOP-related literature.

2 MATERIALS AND METHODS

2.1 Analytical Method Validation

A stock solution of formaldehyde at 1000 mg·L⁻¹ was prepared in distilled and deionized water from a commercial 37% solution (CAS No. 50-00-0, ROTH). A working solution of 20 mg·L⁻¹ was obtained by diluting the stock solution. Both solutions were stored at 4 °C protected from light and were used to calibrate and prepare the synthetic effluents in the analytical and photolytic assays. All analytical procedures used reagent-grade chemicals (P.A.) and ultrapure water to ensure strict matrix control and minimize potential interferences.

A 5% chromotropic acid solution (5 g·100 mL⁻¹) was prepared using the disodium salt of chromotropic acid (4,5-dihydroxynaphthalene-2,7-disulfonic acid; CAS No. 5808-22-0, 98.5%, SIGMA-ALDRICH). The chromogenic reaction, which yields a violet complex between formaldehyde and the reagent under strongly

acidic conditions (Fagnani *et al.*, 2003), had its acidity adjusted to ensure an analytical response within the linear range of the spectrophotometer.

For each determination, 1 mL of sample (or distilled water for the blank) was transferred to 10 mL volumetric flasks. Then, 0.14 mL of the chromotropic acid solution, 3.66 mL of demineralized water, and 5.2 mL of concentrated sulfuric acid (98%, P.A.) were added, performing better than diluted H₂SO₄ (49%). After reaction completion, the solutions were analyzed in a 10-mm quartz cuvette over the wavelength range of 200–800 nm in a Hach UV-Vis spectrophotometer (DR5000). The analytical blank was used to zero the instrument.

The calibration curve was constructed in the range of 0.10–8.00 mg·L⁻¹. Standards up to 2.00 mg·L⁻¹ were prepared from the 20 mg·L⁻¹ working solution, whereas higher concentrations were prepared from the stock solution (1000 mg·L⁻¹). The normality of the repeatability data was assessed on PAST software.

Repeatability (intra-assay precision) was determined by the coefficient of variation from measurements performed on two different days. The limits of detection and quantification were calculated based on the standard deviation of the blank and the slope of the calibration curve following the recommendations of the International Conference On Harmonization – ICH (2005), Instituto Nacional de Metrologia, Qualidade e Tecnologia – INMETRO (2018), and Ribani *et al.* (2004). Relative absorbance variation ($\Delta\text{Abs}\%$) is shown as the difference between the maximum and minimum values after normalization to the maximum absorbance.

2.2 System for pure UV photolysis and H₂O₂-assisted UV photolysis

The experiments were conducted using a synthetic formaldehyde solution (20 mg·L⁻¹)

under pure UV photolysis (UV) or homogeneous photolysis assisted by hydrogen peroxide (UV/H₂O₂), using 35% (w/w) H₂O₂ (Merck or Bernd Kraft, CAS No. 7722-84-1). The pH was adjusted to neutral (≈ 7.0) or acidic (≈ 2.3) using H₂SO₄. The experimental setup (Figure 1) consisted of a 200-mL stainless-steel reactor (1) that

was connected to a recirculation and sampling reservoir (2). Continuous flow was maintained by a peristaltic pump (ISMATEC MCP-Process IP 65, 150 W) operating at 60 mL·min⁻¹, using polytetrafluoroethylene tubing (4). The return flow to the reactor occurred by a drip system (5), ensuring a constant working volume.

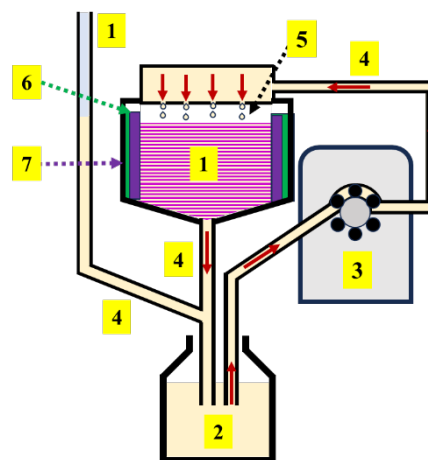
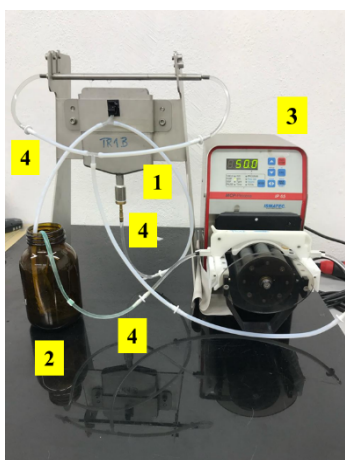


Figure 1 – Formaldehyde Photolysis System at 20 mg·L⁻¹.

Legend: 1. PFR reactor (plug-flow reactor), 2. Recirculation and sampling reservoir, 3. Peristaltic pump, 4. Tubing and fittings, 5. Drip system, 6. UV LED lamps, 7. Radiation diffuser plate.

Overall, five glass diffuser plates (100 × 100 × ≈6 mm) were evaluated (Figure 2A–E):

- A) Bosil (translucent borosilicate),
- B) BosilF60 (borosilicate with laser-modified surface),
- C) BosilF100 (borosilicate with enlarged laser-modified area),
- D) UltraClean (translucent soda-lime glass), and
- E) UltraClean 300 ppi (soda-lime glass with laser micro-engraving).

UV-A LED lamps (SMD-3528; $\lambda \approx 370.8$ nm; 120 LEDs·m⁻¹; 9.6 W·m⁻¹) were used emitting 3.2–3.3 eV photons with a 9.6 mW·cm⁻² nominal irradiance. The diffuser plates were installed in

dedicated slots (Figure 2F–G), ensuring stable positioning. Borosilicate glass showed higher UV-A transmittance and greater thermal stability than soda-lime glass, which justifies their comparison. Overall, two lateral UV sources provided uniform irradiation over a 100-cm² area (10 × 10 cm).

The operational conditions were standardized as follows: a 200-mL reaction volume, 22 °C temperature, initial pH adjusted to neutral or acidic values, a 60-mL·min⁻¹ flow rate, initial concentration of 20-mg·L⁻¹ formaldehyde, and a 20-mg·L⁻¹ H₂O₂ concentration (molar ratio $\approx 0.88:1$). The distance between the liquid surface and the LEDs varied according to plate configuration (Figure 2H–I) under constant irradiance.

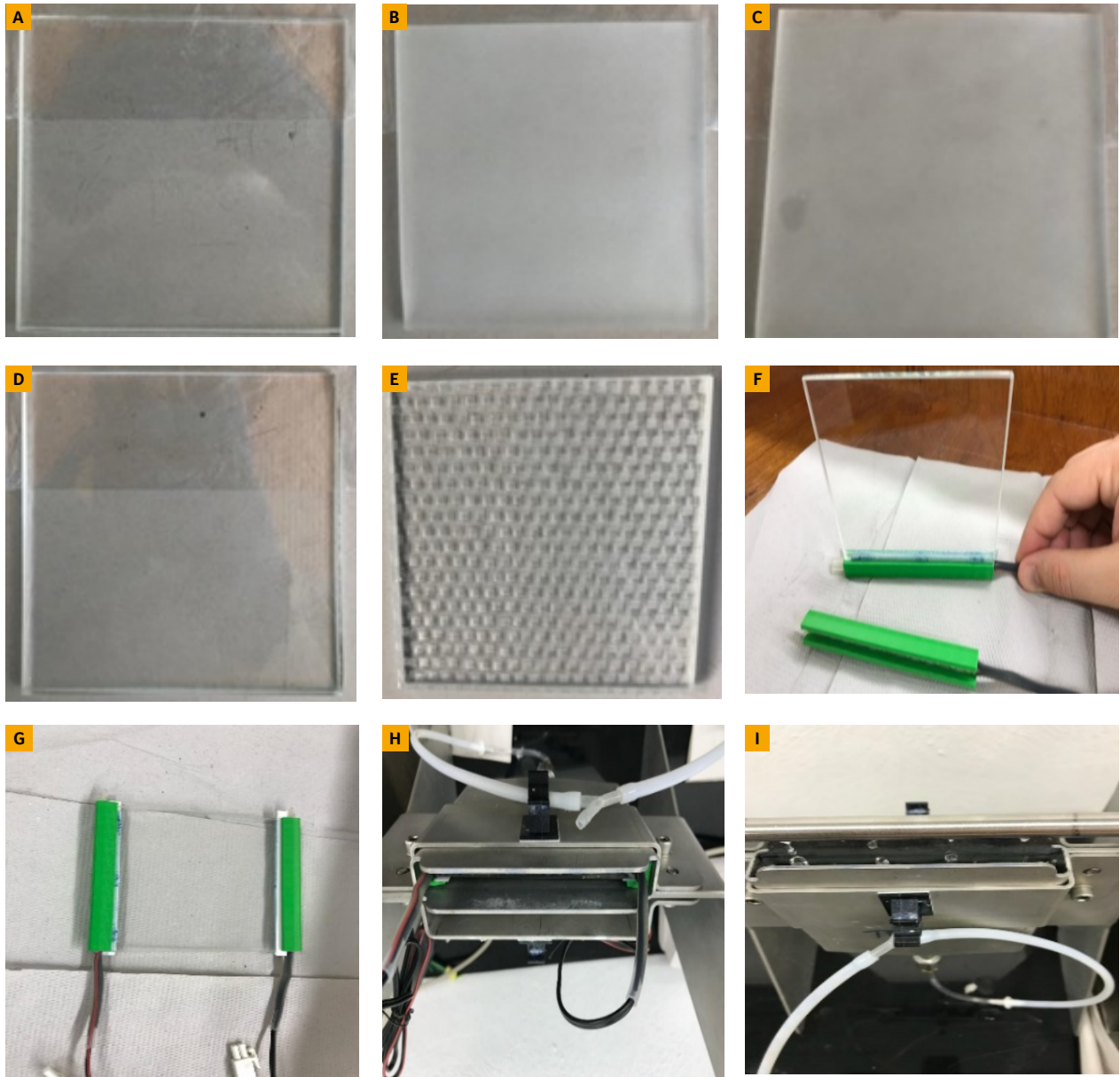


Figure 2 – UV radiation diffuser glass plates and details of plate mounting on the lamp and reactor.

Legend: A: Bosil — B: BosilF60 — C: BosilF100 — D: UltraClean — E: UltraClean 300 ppi — F: plate fitting — G: installed plate — H: reactor light source — I: top view of the drip system.

After filling the reactor and stabilizing the working volume, irradiation with UV-A LEDs (1.2 W, 370.8 nm) was initiated at time zero. The experiments were conducted for up to 300 min at 22 °C, with the initial pH adjusted to neutral or acidic conditions. Samples were collected every 15 min. For the UV/H₂O₂ experiments, 35% (w/w) H₂O₂ was added as required to maintain a concentration

of 20 mg·L⁻¹. Neutral pH was controlled without UV irradiation or H₂O₂, whereas under acidic conditions an additional control containing H₂O₂ without UV irradiation (H₂O₂–OXI) was conducted to isolate chemical oxidation. Concentrations were determined as in Section 2.1 and anomalous data points were excluded based on statistical validation criteria.

3 RESULTS AND DISCUSSION

3.1 Evaluation and Validation of the Analytical Method

3.1.1 Spectrophotometric Characterization and Linearity

The chromogenic reaction between formaldehyde and chromotropic acid under strongly acidic conditions produced an intense purple color, easily visible to the naked eye and useful for identifying experimental deviations. The selected concentration range followed previous studies using values near $5 \text{ mg}\cdot\text{L}^{-1}$ (Cui *et al.*, 2011), which are consistent with the concentrations in industrial effluents—such as those from phenol–formaldehyde resin production—and in environmental accident scenarios.

The absorbance spectrum showed a maximum at 574 nm (Figure 3A), in agreement with values in the literature (Sawicki; Hauser; McPherson, 1962; Shariati-Rad; Irandoust; Mozaffarinia, 2016; Velikonja *et al.*, 1995). The calibration curve showed linear behavior in the $0.10\text{--}4.00 \text{ mg}\cdot\text{L}^{-1}$ range, with $0.065\text{--}2.243$ absorbance values, which is consistent with the operational range of the UV–Vis spectrophotometer used. The resulting linear model ($\text{Abs} = 0.559x + 0.0645$) yielded $R^2 = 0.9946$ (Figure 3B), confirming the concentration–response relationship. Residual analysis showed a random distribution from -0.031 to $+0.025$ Abs, with no systematic trends, and standardized residuals from -1.42 to $+1.33$, indicating the adequacy of the model.

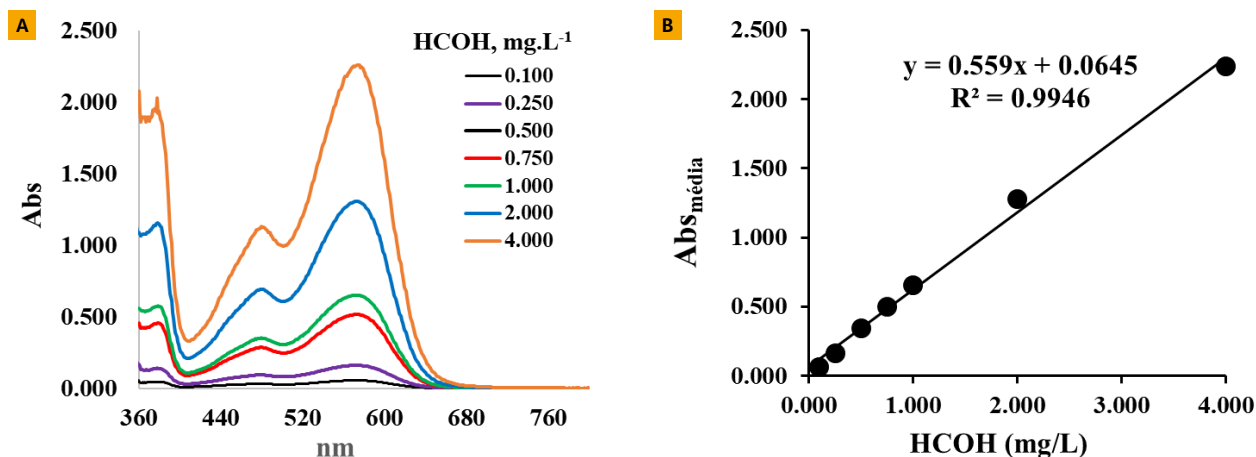


Figure 3 – Analytical validation of the chromotropic acid method to determine formaldehyde.

Legend: A: Absorbance spectra of formaldehyde (HCOH) at varying concentrations ($0.10\text{--}4.00 \text{ mg}\cdot\text{L}^{-1}$), peaking at 574 nm — B: Corresponding calibration curve with linear fit from 0.10 to $4.00 \text{ mg}\cdot\text{L}^{-1}$ ($R^2 = 0.9946$); mean of two measurements.

Table 1 – Calibration parameters and analytical validation of the chromotropic acid method.

Parameter	This study	Shariati-Rad, Irandoust, and Mozaffarinia, 2016
Linear range ($\text{mg}\cdot\text{L}^{-1}$)	0.5–4.0	0.003–7.0
Limit of detection ($\text{mg}\cdot\text{L}^{-1}$)	0.126	0.0050
Limit of quantification ($\text{mg}\cdot\text{L}^{-1}$)	0.382	0.0162
Slope	0.5589	0.3990
Intercept	0.0645	0.0020
Determination coefficient (R^2)	0.9973	0.9810
λ_{max} (nm)	574	574

Legend: Comparison of analytical performance parameters, including linear range, detection and quantification limits, regression coefficients, and maximum absorption wavelength (λ_{max}).

The analytical method showed high sensitivity and linearity in the 0.10–4.00 mg·L⁻¹ range, with 0.126 and 0.382 mg·L⁻¹ detection and quantification limits, respectively—higher than those in Shariati-Rad, Irandoust, and Mozaffarinia (2016) (Table 1). Signal saturation above 4 mg·L⁻¹ confirmed the suitability of the selected linear range for the photolytic and kinetic assays.

Although analytical precision does not necessarily require a normal distribution, it must show consistency and reproducibility. Statistical parameters such as the standard deviation (σ) and coefficient of variation (CV) obtained under controlled conditions (ICH, 2005; Ribani *et al.*, 2004) can evaluate these characteristics. This study analyzed six formaldehyde standard samples (20 mg·L⁻¹) in triplicates, totaling 18 measurements (Table 2), to assess precision. The Shapiro-Wilk test indicated deviation from

normality ($p = 0.02313$), whereas the Lilliefors test yielded $p = 0.1813$, indicating an acceptable distribution for analysis. The minimum (1.361) and maximum (1.420) absorbance values resulted in a 0.059 amplitude. The global mean (1.388) and median (1.387) showed excellent agreement, with a 0.022 overall standard deviation and a 1.58% CV, confirming high precision and repeatability. The relative absorbance variation ($\Delta\text{Abs}\%$) remained below 5.00% for all measurements, meeting the recommended international criteria for precision. These results evince a precise and reproducible method with low dispersion even at fixed concentrations, supporting its suitability for the subsequent kinetic and photolytic experiments. The use of high-purity reagents minimized potential interferences, ensuring adequate analytical selectivity for application in the PFR reactor system.

Table 2 – Assessment of precision and reproducibility of the chromotropic acid method for formaldehyde determination (20 mg·L⁻¹).

Sample	1st measurement	2nd measurement	3rd measurement	Mean Abs (\bar{x})	\bar{x}	Md	CV (%)	$\Delta\text{Abs}\%$
N1	1.364	1.366	1.366	1.365	0.0009	1.366	0.069	-1.68
N2	1.363	1.361	1.362	1.362	0.0008	1.362	0.060	-1.90
N3	1.383	1.382	1.385	1.383	0.0012	1.383	0.090	-0.39
N4	1.389	1.39	1.388	1.389	0.0008	1.389	0.059	0.04
N5	1.411	1.411	1.412	1.412	0.0005	1.411	0.033	1.70
N6	1.420	1.419	1.419	1.419	0.0005	1.419	0.033	2.20

Legend: Results from six standard formaldehyde samples (20 mg·L⁻¹), analyzed in triplicate (18 measurements). Shown are individual absorbance values at 574 nm, means (\bar{x}), standard deviations (σ), medians (Md), coefficients of variation (CV; Equation 1), and relative absorbance variation ($\Delta\text{Abs}\%$). The low dispersion confirms the high precision and reproducibility of the method.

3.1.2 Interferences and Analytical Matrix Control

Since organic and inorganic interferents (Shariati-Rad; Irandoust; Mozaffarinia, 2016) can affect the chromotropic acid method, this study used reagent-grade chemicals (P.A.), ultrapure water, and synthetic effluent to ensure strict matrix control and to minimize

interferences during its photolytic assays. The homogeneous photolysis tests with hydrogen peroxide (H₂O₂) evaluated the addition of sodium sulfate (Na₂SO₄) and ascorbic acid (vitamin C) for the removal of residual peroxide. However, both additives induced undesirable coloration, compromising measurement reliability and precluding their use.

The formation of the characteristic violet coloration of the method requires a strongly acidic medium (Shariati-Rad; Irandoust; Mozaffarinia, 2016). Diluted H_2SO_4 (49% w/w) showed unsatisfactory analytical performance, whereas concentrated H_2SO_4 (98%) provided greater chromogenic intensity and stability. Therefore, all assays used concentrated reagent-grade sulfuric acid, ensuring the reliability of the determinations. Consequently, the technique is suitable only for ultrapure samples and controlled systems, such as the formaldehyde degradation kinetic experiments performed in this study.

3.2 Performance of the UV Photolysis Processes

3.2.1 UV Photolysis at Neutral pH (UV, pH=7.0)

This study evaluated several formaldehyde degradation conditions in a PFR system. Under control conditions (without UV radiation), the formaldehyde concentration remained unchanged (-0.16%), indicating solution stability and the absence of detectable volatilization or non-photoinduced reactions (Table 3). Chemical oxidation with H_2O_2 in the absence of UV (H_2O_2 -OXI) at neutral pH was also negligible.

Table 3 – Formaldehyde removal under several UV photolysis conditions and diffuser materials.

Degradation conditions	W/O UV (control), %	UV-Bosil, %	UV-BosilF60, %	UV-BosilF100, %	UV-UltraClean, %	UV-UltraClean300, %
UV pH=7.0	-0.16	12.72	3.18	0.76	2.69	4.32
UV pH=7.0 H_2O_2	-0.61	6.54	5.24	6.15	5.22	7.27
UV pH=2.3 H_2O_2	14.45	23.37	24.19	20.47	18.16	7.08

Legend: Mean percentage removal of formaldehyde ($\text{mg}\cdot\text{L}^{-1}$) from 4 to and 5 h relative to t_0 . W/O UV = without UV irradiation. Diffuser plates: Bosil, BosilF60, BosilF100 (borosilicate); UltraClean, UltraClean300 (soda-lime). Conditions: neutral pH (=7.0) and acidic pH (=2.3), with and without H_2O_2 .

In UV photolysis without hydrogen peroxide, efficiency depended on the diffuser material (Figure 4A–B; Table 3). The Bosil plate (translucent borosilicate) showed the highest removal (12.72%). BosilF60, UltraClean, and UltraClean300 achieved 2.69%–4.32%, whereas BosilF100 was ineffective (0.76%). These patterns reflect optical properties: translucent

borosilicate provides higher UV transmission and diffusion, whereas laser micro-engraving (F60/F100) increases lateral scattering and backscattering, reducing photon penetration into the liquid. In soda-lime plates (UltraClean/ UltraClean300), the lower UV transmittance accounts for the reduced removals, even with a 10-cm optical path.

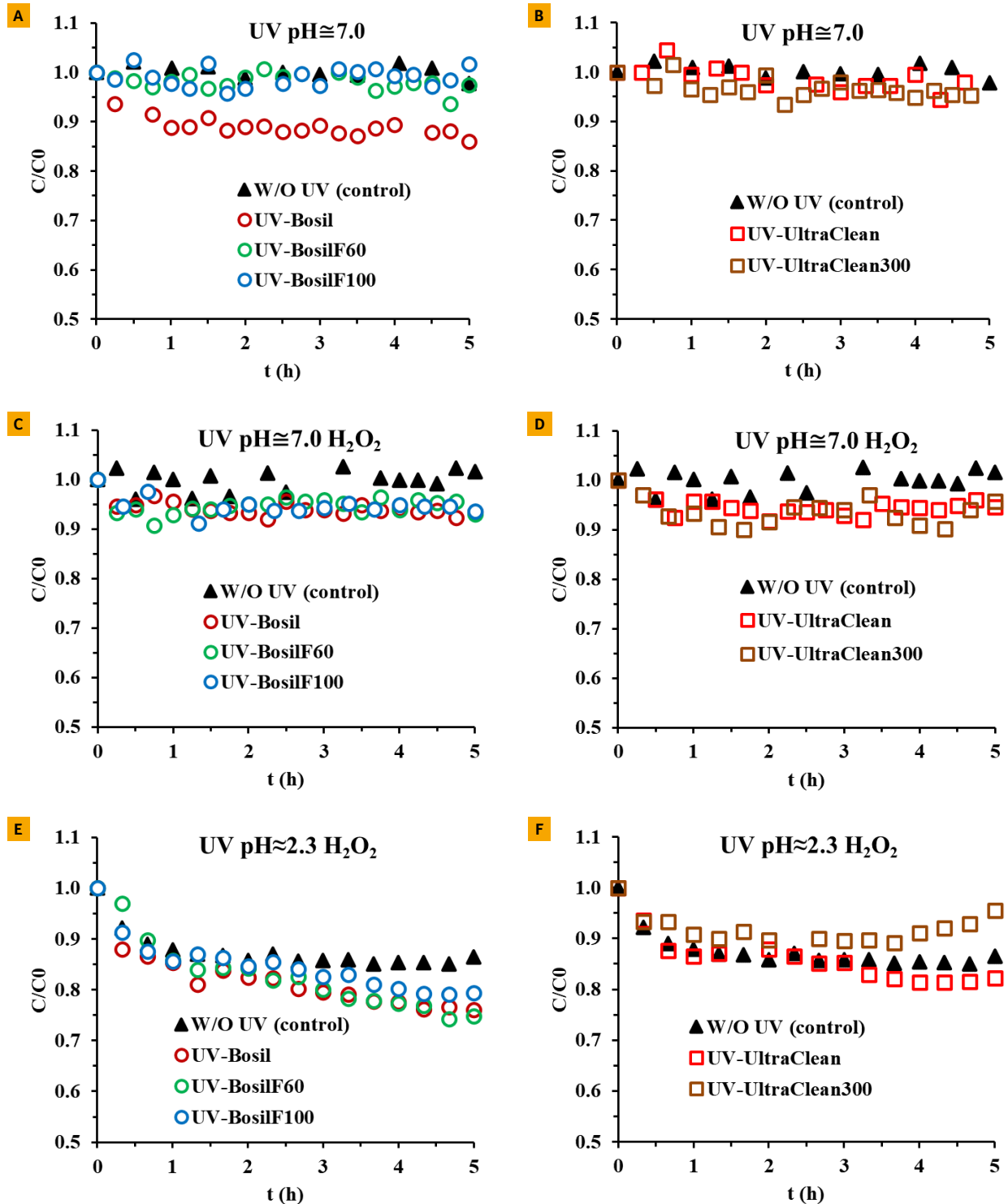


Figure 4 – Time evolution of formaldehyde degradation in the PFR reactor using several diffuser plates under various UV-photolysis conditions.

Legend: A–B: UV photolysis at neutral pH (\approx 7.0) using borosilicate (Bosil, BosilF60, BosilF100) and soda-lime plates (UltraClean, UltraClean300), respectively. C–D: Homogeneous UV/H₂O₂ photolysis at neutral pH with the same materials. E–F: Homogeneous UV/H₂O₂ photolysis at acidic pH (\approx 2.3) for borosilicate and soda-lime plates. C/C₀ = relative formaldehyde concentration; W/O UV = no-UV control. At pH=2.3, the control includes H₂O₂ without UV (direct oxidation, H₂O₂–OXI).

3.2.2 UV/H₂O₂ photolysis at neutral pH (pH=7.0)

H₂O₂-assisted photolysis at neutral pH showed modest removals (Figure 4C–D; Table 3). For the Bosil plate, efficiency decreased to 6.54%, about half the value without H₂O₂. The other plates showed 5.24%–7.27%. These conditions obtained limited •OH generation from H₂O₂, and UV/H₂O₂ did not outperform direct photolysis with Bosil, indicating low radical efficiency under neutral conditions.

3.2.3 UV/H₂O₂ photolysis at acidic pH (pH=2.3)

Acidification significantly increased removal efficiencies (Figure 4E–F; Table 3). Chemical oxidation by hydrogen peroxide in the absence of UV (H₂O₂–OXI) reached 14.45%. In the acidic control containing H₂O₂ but no UV (H₂O₂–OXI; Table 3), the reduction in C/C₀ results from direct chemical oxidation by peroxide under strongly acidic conditions. In this medium, formaldehyde is converted to HCOOH, followed by mineralization to CO₂, as widely reported in the literature (Mattos *et al.*, 2003; Dalponte *et al.*, 2016). This behavior corroborates the 14.45% mean for H₂O₂–OXI and clearly distinguishes chemical losses from potential physical losses (e.g., volatilization), which tend to be lower under acidic conditions.

Under UV/H₂O₂ conditions, the highest removals occurred with BosilF60 (24.19%) and Bosil (23.37%), followed by BosilF100 (20.47%) and UltraClean (18.16%). UltraClean300 showed the lowest performance (7.08%). The observed enhancement is associated with increased hydroxyl radical generation in acidic media, improved oxidant stability, and greater availability of reactive radicals.

Moreover, in acidic environments, formaldehyde shows greater relative stability, reducing volatilization losses. However, under neutral or alkaline conditions the equilibrium between free formaldehyde and its hydrated form (methylene glycol) shifts toward the release of more free formaldehyde (Winkelman *et al.*, 2002).

No previous assay had observed this phenomenon (–0.16% and –0.61%; Table 3).

3.2.4 Synthesis of trends and role of the diffuser

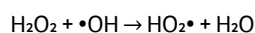
The results confirm that the diffuser material is a key determinant of photochemical efficiency. Borosilicate plates—particularly Bosil and BosilF60—outperformed soda-lime plates under most conditions due to their higher transmittance and improved photon utilization. The pH levels also played a critical role: UV/H₂O₂ showed substantial gains under acidic conditions but limited enhancement at neutral pH. Geometric and optical characteristics strongly influenced the transmission/backscattering balance; laser-microtextured surfaces (F60/F100) may either increase or decrease efficiency, and, in the case of BosilF100, excessive diffusion compromised photon penetration.

3.2.5 Comparison with literature

This study (maximum of 24.19% for UV/H₂O₂–BosilF60 under acidic conditions) found lower yields than those reported for conventional batch systems. Kajitvichyanukul *et al.* (2006) observed removals above 90% at pH=3 using high doses of H₂O₂ and high-intensity mercury lamps (254 nm). Similarly, Guimarães *et al.* (2012) reported removals exceeding 80% using a molar H₂O₂:HCHO ratio of 4:1 under acidic conditions, whereas Mattos *et al.* (2003) highlighted the strong influence of pH and oxidant concentration on process performance. In contrast, this study used low-power UV-A LEDs (370.8 nm), a ≈0.88:1 H₂O₂:HCHO molar ratio, a short residence time, and a PFR, conditions that result in lower photon flux and degradation efficiency.

In addition to methodological differences, the lower efficiency in homogeneous photolysis assisted by H₂O₂ (UV/H₂O₂), particularly at neutral pH, can be explained by classical mechanisms of advanced oxidation processes. Excess H₂O₂ causes the peroxide to scavenge hydroxyl radicals (•OH)

(as in the reaction below), generating less reactive peroxy species ($\text{HO}_2\cdot/\text{O}_2\cdot^-$) and decreasing the effective availability of radicals for formaldehyde oxidation (Bolton; Cater, 1994; Büyüksahin, 2017).



Recombination and non-radical decomposition pathways also predominate at neutral pH, reducing overall efficiency (De Laat; Le; Legube, 2005; Glaze; Kang; Chapin, 1987), whereas the photolysis of H_2O_2 is more effective in acidic media, yielding a higher quantum efficiency for $\cdot\text{OH}$ production.

Another relevant factor is the inner-filter effect from absorption and optical backscattering at the reactor-diffuser plate-solution interface, which attenuates light penetration and lowers the rate of radical photogeneration (Bolton; Linden, 2003). Moreover, non-radical decomposition catalyzed by impurities and radical scavenging by inorganic species or by H_2O_2 diverts oxidants from the target substrate, further compromising performance (De Laat; Le; Legube, 2004).

These mechanisms and the used operational conditions explain the lower efficiencies than in batch studies such as Dalponte *et al.* (2016), Shariati-Rad, Irandoust, and Mozaffarinia (2016), and Nurely *et al.* (2021), which obtained yields of 50%–70% using high H_2O_2 doses, longer residence times, and high-intensity UV sources. Such differences arise from hydrodynamics, radiation field distribution, oxidant dosage, and wavelength (370.8 nm in this study vs. 254 nm in others), all of which directly affect the photodecomposition rate of H_2O_2 and $\cdot\text{OH}$ generation.

Nevertheless, PFRs offer important operational advantages—such as continuous-mode operation and potential for industrial scale-up—if factors such as diffuser type, pH conditions, and the H_2O_2 -to-substrate ratio are optimized to maximize photon efficiency and minimize optical and chemical losses.

3.2.6 Practical implications and recommendations

The results indicate that the choice of material and operational conditions is essential to optimize performance. Processes should prioritize borosilicate diffuser plates, particularly Bosil and BosilF60, as diffusers in PFRs. Acidic conditions with carefully controlled peroxide dosages enhance UV/ H_2O_2 efficiency. Reactor geometry and photon distribution require evaluations to minimize optical losses and maximize the generation of reactive species. Moreover, practical applications require consideration of costs and safety associated with acidification and the use of H_2O_2 .

4 CONCLUSIONS

The chromotropic-acid method proved suitable for monitoring formaldehyde degradation, offering high precision, good linearity, and a detection limit compatible with model-solution assays. Concentrated H_2SO_4 (98%) increased chromogenic intensity and stability, and the method showed low dispersion and high reproducibility, fulfilling international validation criteria. Nonetheless, its applicability to real environmental matrices remains limited as inorganic and organic interferences may reduce selectivity and affect spectrophotometric measurements. Moreover, its detection limit may be inadequate for the trace-level concentrations typically found in surface waters and treated effluents, requiring more sensitive techniques or additional matrix pre-treatment.

Formaldehyde degradation in the plug-flow reactor was strongly influenced by pH and diffuser type. At neutral pH, removals were low (up to 12.72% with UV-Bosil), and UV/ H_2O_2 offered no significant gain. In acidic medium, efficiency increased (up to 24.19% with UV/ H_2O_2 -BosilF60) due to greater hydroxyl-radical production. Borosilicate plates (Bosil and BosilF60) consistently outperformed soda-lime

glass ones, supporting their selection as preferred materials for improving photochemical performance.

Future research should perform tests with real effluents containing typical environmental interferences to validate performance under complex conditions. Further optimization of the H₂O₂:HCHO molar ratio and pH control would maximize radical generation, reduce oxidant losses, and improve the practical applicability of the technology.

The results show that key parameters—pH, diffuser glass type, and UV intensity—directly influence process efficiency. Therefore, evaluating alternative reactor configurations (e.g., longer residence time, better photon distribution, or hybrid systems such as UV-Fenton or UV-TiO₂) and radiation sources of different wavelengths (e.g., UV-C or high-power LEDs) configure a sound strategy to improve efficiency and scalability. Such advances would strengthen the robustness and practical applicability of homogeneous UV/H₂O₂ photolysis for treating formaldehyde-containing waters and effluents.

5 AUTHOR CONTRIBUTIONS

Conceptualization: Lima TM, Otto N, and Mathias AL; **Methodology:** Lima TM and Otto N; **Investigation:** Lima TM and Otto N; **Writing – original draft, review, and editing:** Lima TM, Otto N, and Mathias AL; **Resources:** Mathias AL.

6 ACKNOWLEDGEMENTS

TM de Lima gratefully acknowledge Prof. Dr. Uwe Bernd Menzel, retired professor at the Institute for Sanitary Engineering, Water Quality and Solid Waste Management at the University of Stuttgart, for enabling the DAAD scholarship that made the development of this research in Germany possible. TM de Lima and AL Mathias acknowledge the Federal University of Paraná (UFPR) for the academic and research infrastructure essential to the development of this study.

7 FUNDING

DAAD – Deutscher Akademischer Austauschdienst (scholarship made available by Prof. Dr. Uwe Bernd Menzel).

8 REFERENCES

- BESSAIRE, T. *et al.* Artefact formation of formaldehyde in milk powders: Impact of analytical conditions. **Food Control**, [s. l.], v. 93, p. 23–31, 2018. doi: <https://doi.org/10.1016/j.foodcont.2018.05.029>.
- BOLTON, J. R.; CATER, S. R. Homogeneous photodegradation of pollutants in contaminated water: an introduction. In: HELZ, G. R.; ZEPP, R. G.; CROSBY, D. G. (Orgs.). **Aquatic Surface Photochemistry**. Boca Raton: CRC Press, 1994. p. 467–490.
- BOLTON, J. R.; LINDEN, K. G. Standardization of methods for fluence determination in bench-scale UV experiments. **Journal of Environmental Engineering**, Reston, v. 129, n. 3, p. 209–215, 2003. doi: [https://doi.org/10.1061/\(ASCE\)0733-9372\(2003\)129:3\(209\)](https://doi.org/10.1061/(ASCE)0733-9372(2003)129:3(209)).
- CUI, D.-D. *et al.* Removal of formaldehyde from aqueous solutions using TiO₂ immobilized on bamboo activated carbon. **Journal of Functional Materials**, [s. l.], v. 42, p. 438–441, 2011.
- DALPONTE, I. *et al.* Remoção de Poluentes utilizando Processos Oxidativos Avançados. In: KOLICHESKI, M. B. *et al.* (Orgs.). **Meio Ambiente Urbano e Industrial: Soluções, Tecnologias e Estratégias Aplicadas à Gestão**. Curitiba: UFPR; SENAI; Universität Stuttgart, 2016. p. 15–35.
- DE LAAT, J.; LE, G. T.; LEGUBE, B. A comparative study of the effects of chloride, sulfate and nitrate ions on the rates of decomposition of H₂O₂ and organic compounds by Fe(II)/H₂O₂ and Fe(III)/H₂O₂. **Chemosphere**, [s. l.], v. 55, n. 5, p. 715–723, 2004. doi: <https://doi.org/10.1016/j.chemosphere.2003.11.021>.
- DELIKHOON, M. *et al.* Characteristics and health effects of formaldehyde and acetaldehyde in an urban area in Iran. **Environmental Pollution**, [s. l.], v. 242, p. 938–951, 2018. doi: <https://doi.org/10.1016/j.envpol.2018.07.037>.
- FAGNANI, E. *et al.* Chromotropic acid-formaldehyde reaction in strongly acidic media. The role of dissolved oxygen and replacement of concentrated sulphuric acid. **Talanta**, [s. l.], v. 60, n. 1, p. 171–176, 2003. doi: [https://doi.org/10.1016/S0039-9140\(03\)00121-8](https://doi.org/10.1016/S0039-9140(03)00121-8).
- GASPARINI, F. *et al.* A simple and green analytical method for the determination of formaldehyde. **Journal of the Brazilian Chemical Society**, [s. l.], v. 19, n. 8, 2008. doi: <https://doi.org/10.1590/S0103-50532008000800012>.
- GHANI, A. *et al.* Reducing formaldehyde emission of urea formaldehyde-bonded particleboard by addition of amines

- as formaldehyde scavenger. **Building and Environment**, [s. l.], v. 142, p. 188-194, 2018. doi: <https://doi.org/10.1016/j.buildenv.2018.06.020>.
- GLAZE, W. H.; KANG, J.-W.; CHAPIN, D. H. The chemistry of water treatment processes involving ozone, hydrogen peroxide and ultraviolet radiation. **Ozone: Science & Engineering**, [s. l.], v. 9, n. 4, p. 335-352, 1987. doi: <https://doi.org/10.1080/01919518708552148>.
- GONZALEZ-GIL, G.; KLEEREBEZEM, R.; LETTINGA, G. Conversion and toxicity characteristics of formaldehyde in acetoclastic methanogenic sludge. **Biotechnology and Bioengineering**, [s. l.], v. 79, n. 3, p. 314-322, 2002. doi: <https://doi.org/10.1002/bit.10294>.
- GUIMARÃES, J. R. *et al.* Degradation of formaldehyde by advanced oxidation processes. **Journal of Environmental Management**, [s. l.], v. 107, p. 96-101, 2012. doi: <https://dx.doi.org/10.1016/j.jenvman.2012.04.024>.
- HLADOVÁ, M. *et al.* Review of Spectrophotometric Methods for Determination of Formaldehyde. **Research Papers**, [s. l.], v. 27, n. 44, p. 105-120, 2019.
- ICH – INTERNATIONAL CONFERENCE ON HARMONIZATION. **Validation of Analytical Procedures: Text and Methodology Q2 (R1)**. Geneva: ICH, 2005.
- INMETRO – INSTITUTO NACIONAL DE METROLOGIA, QUALIDADE E TECNOLOGIA. **DOQ-CGCRE-008**. Brasília, DF: Inmetro, 2018.
- JOHARI, M. A. M. *et al.* Microbottle resonator for formaldehyde liquid sensing. **Optik**, [s. l.], v. 173, p. 180-184, 2018. doi: <https://doi.org/10.1016/j.ijleo.2018.08.022>.
- KADEN, D. A. *et al.* Formaldehyde. In: WORLD HEALTH ORGANIZATION (Org.). **WHO guidelines for indoor air quality: selected pollutants**. Copenhagen: WHO, 2010. p. 103-156.
- KAJITVICHYANUKUL, P. *et al.* Degradation and detoxification of formaline wastewater by advanced oxidation processes. **Journal of Hazardous Materials**, [s. l.], v. 135, n. 1-3, p. 337-343, 2006. doi: <https://doi.org/10.1016/j.jhazmat.2005.11.071>.
- LARSEN, D. 2.12: Absorption Spectrum of Formaldehyde. **LibreTexts**, 2024. Available from: <https://is.gd/eZbyRr>. Access in: Mar 20, 2026.
- LUGWISHA, E. H. J.; MAHUGIJA, J. A. M.; MWANKUNA, C. Levels of formaldehyde and acetaldehyde in selected bottled drinking water sold in urban areas in Tanzania. **Tanzania Journal of Science**, [s. l.], v. 42, p. 1-14, 2016.
- MATTOS, I. L. *et al.* Peróxido de hidrogênio: importância e determinação. **Química Nova**, Campinas, v. 26, n. 3, p. 373-380, 2003. doi: <https://doi.org/10.1590/S0100-40422003000300015>.
- NURLELY *et al.* Potentiometric enzyme biosensor for rapid determination of formaldehyde based on succinimide-functionalized polyacrylate ion-selective membrane. **Measurement**, [s. l.], v. 175, p. 109112, 2021. doi: <https://doi.org/10.1016/j.measurement.2021.109112>.
- REINGRUBER, H.; PONTEL, L. B. Formaldehyde metabolism and its impact on human health. **Current Opinion in Toxicology**, [s. l.], v. 9, p. 28-34, 2018. doi: <https://doi.org/10.1016/j.cotox.2018.07.001>.
- RIBANI, M. *et al.* Validação em métodos cromatográficos e eletroforéticos: Revisão. **Química Nova**, Campinas, v. 27, n. 5, p. 771-780, 2004. doi: <https://doi.org/10.1590/S0100-40422004000500017>.
- SAWICKI, E.; HAUSER, T. R.; MCPHERSON, S. Spectrophotometric Determination of Formaldehyde and Formaldehyde-Releasing Compounds with Chromotropic Acid, 6-Amino-1-naphthol-3-sulfonic Acid (J Acid), and 6-Anilino-1-naphthol-3-sulfonic Acid (Phenyl J Acid). **Analytical Chemistry**, [s. l.], v. 34, n. 11, p. 1460-1464, 1962. doi: <https://doi.org/10.1021/ac60191a033>.
- SHARIATI-RAD, M.; IRANDOUST, M.; MOZAFFARINIA, N. Response Surface Methodology in Spectrophotometric Determination of Formaldehyde Using Chromotropic Acid. **Analytical Bioanalytical Chemistry Research**, [s. l.], v. 3, n. 2, p. 149-157, 2016. doi: <https://doi.org/10.22036/abcr.2016.15302>.
- VAKYLABAD, A. B. Treatment of highly concentrated formaldehyde effluent using adsorption and ultrasonic dissociation on mesoporous copper iodide (CuI) nano-powder. **Journal of Environmental Management**, [s. l.], v. 285, , 2021. doi: <https://doi.org/10.1016/j.jenvman.2021.112085>.
- VELIKONJA, Š. *et al.* Comparison of gas chromatographic and spectrophotometric techniques for the determination of formaldehyde in water. **Journal of Chromatography A**, [s. l.], v. 704, n. 2, p. 449-454, 1995. doi: [https://doi.org/10.1016/0021-9673\(95\)00049-5](https://doi.org/10.1016/0021-9673(95)00049-5).
- WINKELMAN, J. G. M. *et al.* M. Kinetics and chemical equilibrium of the hydration of formaldehyde. **Chemical Engineering Science**, [s. l.], v. 57, n. 19, p. 4067-4076, 2002. doi: [https://doi.org/10.1016/S0009-2509\(02\)00358-5](https://doi.org/10.1016/S0009-2509(02)00358-5).
- WHO – WORLD HEALTH ORGANIZATION. **Background document for development of WHO Guidelines for Drinking-water Quality: Formaldehyde in Drinking-water**. Copenhagen: WHO, 2005.
- YU, H. *et al.* Enhanced formaldehyde sensing performance based on Ag@WO₃ 2D nanocomposite. **Powder Technology**, [s. l.], v. 343, p. 1-10, 2019. doi: <https://doi.org/10.1016/j.powtec.2018.11.008>.